AIMS Mathematics, 9(8): 21144–21176.
DOI: 10.3934/math.20241027
Received: 29 February 2024
Revised: 01 June 2024
Accepted: 05 June 2024
Published: 01 July 2024

http://www.aimspress.com/journal/Math

*Research article*

# Exploration of solitons and analytical solutions by sub-ODE and variational integrators to Klein-Gordon model

**Syed T. R. Rizvi[1], Sana Ghafoor[1], Aly R. Seadawy[2], Ahmed H. Arnous[3], Hakim AL Garalleh[4,*] and Nehad Ali Shah[5]**

[1] Department of Mathematics, COMSATS University Islamabad, Lahore Campus, Pakistan

[2] Mathematics Department, Faculty of Science, Taibah University, Al-Madinah Al-Munawarah, 41411, Kingdom of Saudi Arabia

[3] Department of Engineering Mathematics and Physics, Higher Institute of Engineering, El-Shorouk Academy-11837, Egypt

[4] Department of Mathematical Science, College of Engineering, University of Business and Technology, Jeddah 21361, Saudi Arabia

[5] Department of Mathematics, Saveetha School of Engineering, SIMATS, Chennai, 602105, Tamilnadu, India

* **Correspondence:** Email: h.algaralleh@ubt.edu.sa.

**Abstract:** In this paper, we use the sub-ODE method to analyze soliton solutions for the renowned nonlinear Klein-Gordon model (NLKGM). This method provides a variety of soliton solutions, including three positive solitons, three Jacobian elliptic function solutions, bright solitons, dark solitons, periodic solitons, rational solitons and hyperbolic function solutions. Applications for these solitons can be found in optical communication, fiber optic sensors, plasma physics, Bose-Einstein condensation and other areas. We also study some numerical solutions by using forward, backward, and central difference techniques. Moreover, we discuss variational integrators (VIs) using the projection technique for NLKGM. We develop a numerical solution for NLKGM using the discrete Euler lagrange equation, the Lagrangian and the Euler lagrange equation. At the end, in various dimensions, covering 3D, 2D, and contour, we will also plot several graphs for the obtained NLKGM solutions. A contour plot is a type of graphic representation that displays a three-dimensional surface on a two-dimensional plane by using contour lines. Each contour line in the plotted function represents one of the function's constant values, mapping the function's value across the plane. This model has been studied across multiple soliton solutions using various methods in the open literature, but this model for VIs and finite deference scheme (FDS) is the first time it has been studied. Within the various numerical techniques accessible for solving Hamiltonian systems, variational integrators distinguish themselves because of their symplectic quality. Here are some of the symplectic properties:

symplectic orthogonality, energy conservation, area preservation, and structure preservation.

**Keywords:** integrability; variational integrators; nonlinear Klein-Gordon model (NLKGM)
**Mathematics Subject Classification:** 35A09, 35A24, 35C08

## 1. Introduction

One special kind of nonlinear wave is the soliton, which maintains its form and amplitude while passing through a material without dissipating or spreading. We investigated this model for VIs and FDS for the first time; however, it has been studied across numerous soliton solutions using different techniques. A class of numerical methods known as FDS is used in numerical analysis to solve differential equations and approximate derivatives by using finite differences. FDS can convert ordinary differential equations (ODEs) and partial differential equations (PDEs), which may or may not be nonlinear, into a system of linear equations that can be solved using matrix algebra techniques. VIs are geometric numerical techniques where the action integral is derived using the system's Lagrangian. With the aid of the Hamiltonian principle, VIs discretized the Lagrangian to generate a discrete Euler–Lagrange equation. VIs are well known for their ability to display desired long-term energy properties while maintaining a distinct multi-symplectic structure. Zabusky and Kruskal have observed unusual nonlinear interactions between dispersing solitary-wave pulses in nonlinear media [1]. Solitons play an important role in many fields of science and engineering, including nonlinear physics, optics, and fluid dynamics. Solitons are helpful in optical fiber communication systems since they don't produce distortion or interference in optics while transferring data over long distances. Soliton solutions and stable, confined wave solutions to nonlinear evolution equations are fundamental tools for understanding complex processes in physics and mathematics. The Korteweg–de Vries (KdV) equation, which explains the evolution of one-dimensional dispersive waves, is a prime example. KdV solitons, or soliton solutions, are solitary waves that, while propagating, keep their shape and speed. The nonlinear Schrödinger equation (NLSE), which occurs in several disciplines, including optics, is another significant example. Optical solitons are the result of soliton solutions to the NLSE in optics. The behavior of solitons in a system with nonlinear interactions is also described by the Sine–Gordon equation. Soliton structures are stable topological formations that arise in a range of physical situations, including condensed matter physics and are described in the Sine–Gordon equation. Darvishi et al. studied some nonlinear logarithmic equations and obtained Gaussons for them [2]. Akinyemi et al. studied localized wave and oceanic soliton solutions for the variable coefficient equation NLEE [3]. Akinyemi et al. studied coupled NLSKdVE to obtained optical soliton solutions [4]. Senol et al. studied dimensional conformable KP and KPBBM equations to obtained Novel soliton solutions [5]. These examples show the close relationship between solitons and NLEEs, and shed light on the dynamics of waves and fields across a wide range of scientific subjects. These examples also explain how solitons emerge as exceptional solutions in nonlinear system (NLS). Among these equations additional examples of integrable (NLS) with soliton solutions include the Davey-Stewartson, Fokas-Lenells and modified Korteweg-de Vries (mKdV) equations. The combined representation of these equations captures the wide and various landscapes of nonlinear evolution occurrences in several scientific fields. These equations have applications in plasma physics (Zakharov–Kuznetsov equation)

and the study of shallow water waves (Boussinesq equation). Among these equations, one of the renowned model is NLKGM, which was on the name of two famous physicists Oskar Klein and Walter Gordon, and this model discusses relativistic electrons. The well-known NLKGM, is as follows:

$$\wp_{tt} - \alpha^2 \wp_{xx} + \beta\wp - \gamma\wp^2 = 0, \tag{1.1}$$

This equation explains the behavior of a function $\wp(x, t)$ in relation to time $t$ and space $x$, whereby $\wp(x, t)$ can be said to the unknown function that is dependent on the temporal $t$ and spatial $x$ coordinates. $\wp_{tt}$ is $\wp's$ second partial derivative, explains the function's acceleration with regard to time, $\wp_{xx}$ is $\wp's$ second partial derivative, in terms of spatial position, it characterizes the curvature or variations of the function, $\alpha$ is the second-order spatial dispersion and $\gamma$ is the coefficient of quadratic nonlinearity [6].

Soon after Klein's studies were completed, in 1926, Vladimir Fock also independently found the equation. Younas et al. studied the modified nonlinear Schrödinger equation, utilizing a conformable fractional derivative, to obtained diverse exact solutions [7]. Santo et al. examined Klein-Gordon type Cauchy problems with a time-dependent singular potential [8]. According to NLKGM, the Higgs boson a spin-zero component was the first ostensibly elementary particle to be detected. The Higgs boson was discovered as the European organization for nuclear research, or CERN. A number of techniques for discrete KGMs with zero static Peierls-Nabarro potential have been reviewed by Bebikhov et al. Additionally, they mentioned the conserved principles to discrete potential [9]. NLKGM with time-dependent coefficients have been studied for $L_p - L_q$ decay estimates by Hirosawa and Reissing [10]. They clarified how $L_p|L_q$ decay estimations are affected by the relationship between the mass term and the wave propagation speed. In the mass of a linear KGM, Böhme and Reissig have explained the interaction between a diminishing and an oscillating part of a time-dependent coefficient [11].

In this paper, we will study NLKGM with the help of sub-ODE approach. The main concepts of the sub-ODE method are that the traveling wave solutions of a complex nonlinear wave equation can be built using the sub-ODEs or simple and solvable ODEs as solutions. Numerous solutions are provided by this, we obtain periodic, rational, bright, and dark soliton solutions, as well as Weierstrass elliptic function solutions, three positive soliton solutions, three Jacobian elliptic function solutions and hyperbolic function solutions. The sub-ODE method was used by many authors to study a variety of models. In order to create optical solitons and other solutions for fiber Bragg gratings, Zayed et al. used dispersive reflectivity with a quadratic-cubic index of nonlinear refraction, the recently developed sub-ODE technique has been applied. Projective Riccati equations, Jacobi elliptic equations and Riccati equations are some of the sub-ODEs that were frequently utilized [12].

We will also study the NLKGM for VIs. Firstly, the lagrangian density for NLKGM will be examined. This model has been developed in Hamiltonian form, which identifies the Hamiltonian function that controls the dynamics. Next, a chosen time-stepping methodology is used to discretize the continuous time domain and techniques such as finite elements or finite differences are used to discretize the spatial domain. Next, the action integral can be discretized and thus, dynamics can be captured by deriving discrete equations of motion by the application of the variational principle. VIs are numerical methods for solving Hamilton's equations of motion, which show the positions and velocities of physical systems as they change, in classical mechanics. This edition of a well-known classic volume, published by one of the leading experts in this field, John Butcher, contributed to the development and regeneration of the study of numerical methods for solving ordinary differential

equations [13]. With a focus on variational integrators, Leimkuhler and Reich offered a more thorough framework for understanding Hamiltonian dynamics [14]. The Hamiltonian notion of stationary action was utilized by VIs to discretize the Lagrangian and derive a discrete Euler Lagrange equation. Several projection methods for degenerate Lagrangian systems with variational integrators were introduced and compared by Kraus [15]. They derive from a Lagrangian function that characterizes the kinetic and potential energy of the system and are founded on the principle of least action. Compared to conventional numerical approaches, VIs offer many kinds of advantages, including long-term stability, energy conservation, and symplectic preservation. In their study of geometric numerical methods, Hairer et al. explained how to maintain the structures of ODEs [16]. Reich and Cotter investigated the application of variational integrators in wave energy propagation to illustrate their applicability [17]. They play an important role in numerous fields, including computer graphics, engineering, and physics. Lew improved our knowledge of the theoretical foundations of variational integrators and established the idea of discrete variational Hamiltonian mechanics [18]. A mathematical model that depicts how a system changes over time is called a dynamical system (DS). The numerical techniques maintain the physical laws of the original dynamical system [19]. A Lagrangian system is a visualization of a dynamic system, the Lagrangian function describes the system's total energy. The Lagrangian function is applied to determine the system's equations of motion, which demonstrate how the system has evolved over time. The Euler-Lagrange equation is generated with the help of the Lagrangian density. The approach is widely utilized in the fields of quantum mechanics, field theory and classical mechanics, among various other areas of physics. A Hamiltonian function or mathematical assertion that measures the total energy of the system in terms of its position and velocity variables, specifies a particular kind of DS known as a Hamiltonian system. The system's equations of motion are determined by applying the concept of the Hamiltonian function. Farukh et al. exploited the discrete gradient technique when working on the SIRI epidemic model [20]. Butcher et al. explored the properties of G-symplectic methods theoretically and computationally [21]. A geometric-variational approach to field theories and continuous and discrete mechanics was introduced by Marsden and Patrick [22]. Kraus conducted research on the development of variational integrators for numerous key models in plasma physics, including ideal magnetohydrodynamics (plasma fluid theory), the Vlasov-Poisson system (kinetic theory), and guiding center dynamics (particle dynamics). Physical conservation laws such as momentum and energy conservation are given special consideration [23]. A Hamiltonian theory that is canonically chosen to match with the theory of discrete Lagrangian mechanics has been presented by Lall and West [24].

The remaining paper is organized as follows. We will go over the sub-ODE technique in Section 2. The sub-ODE approach will then be used in Section 2.1 to determine the various solutions. The finite difference approach for obtaining numerical solutions for NLKGM will be covered in Section 3. After that, we will discuss the Lagrangian approach to NLKGM in Section 4. We will explain the results and discussions for this model before providing a conclusion.

## 2. Analysis of sub-ODE approach

Using this method, we will assume that the formal solution to Eq (1.1) is:

$$\varphi(\varsigma) = \rho\Re^n(\varsigma),\ \rho > 0, \tag{2.1}$$

where $\varsigma = x - vt$, and $v$ has to be calculated as a non-zero constant to indicate the soliton's velocity, while $\varphi(\varsigma)$ is a real function that depicts the soliton's pulse structure. Here, the equation is satisfied by $\Re(\varsigma)$, where $n$ is a parameter:

$$\Re'^2(\varsigma) = L\Re^{2-2P}(\varsigma) + M\Re^{2-P}(\varsigma) + N\Re^2(\varsigma) + O\Re^{2+p}(\varsigma) + T\Re^{2+2p}(\varsigma),\ p > 0, \tag{2.2}$$

here $L, M, N, O$ *and* $T$ are constants. We determine $n$ in Eq (2.1) by using the homogeneous balance method as follows:

$$K(\varphi) = n,\ \ K(\varphi^2) = 2n, ... \qquad \textit{and} \qquad K(\varphi') = n + p,\ \ K(\varphi'') = n + 2p, .... \tag{2.3}$$

It is widely acknowledged that Eq (2.2) provides solutions for the following cases [12]:

2.0.1. Case 1

If $L = M = O = 0$, substitute in Eq (2.2), we get bright soliton solution for Eq (1.1):

$$\Re(\varsigma) = \left(\sqrt{-\frac{N}{T}}\text{sech}(\sqrt{N}p\varsigma)\right)^{\frac{1}{p}},\ N > 0,\ T < 0, \tag{2.4}$$

a periodic solution

$$\Re(\varsigma) = \left(\sqrt{-\frac{N}{T}}\text{sec}(\sqrt{-N}p\varsigma)\right)^{\frac{1}{p}},\ N < 0,\ T > 0, \tag{2.5}$$

and a rational solution

$$\Re(\varsigma) = \left(\frac{\varepsilon}{\sqrt{T}p\varsigma}\right)^{\frac{1}{p}},\ N = 0,\ T > 0,\ \varepsilon = \pm 1. \tag{2.6}$$

2.0.2. Case 2

If $M = O = 0,\ L = \frac{N^2}{4T}$, substitute in Eq (2.2), we get dark soliton solution for Eq (1.1):

$$\Re(\varsigma) = \left(\varepsilon\sqrt{-\frac{N}{T}}\tanh(\sqrt{N}p\varsigma)\right)^{\frac{1}{p}},\ N > 0,\ T < 0,\ \varepsilon = \pm 1, \tag{2.7}$$

and a periodic solution

$$\Re(\varsigma) = \left(\varepsilon\sqrt{-\frac{N}{T}}\tan(\sqrt{-N}p\varsigma)\right)^{\frac{1}{p}},\ N < 0,\ T > 0,\ \varepsilon = \pm 1. \tag{2.8}$$

2.0.3. Case 3

If $M = O = 0$, substitute in Eq (2.2), we get three Jacobian elliptic function solutions for Eq (1.1):

$$\mathfrak{R}(\varsigma) = \left( \sqrt{-\frac{Nm^2}{T(2m^2-1)}}\, cn\left( \sqrt{\frac{N}{2m^2-1}} p\varsigma \right) \right)^{\frac{1}{p}}, \quad N > 0, \quad L = \frac{N^2 m^2 (m^2-1)}{T(2m^2-1)^2}, \tag{2.9}$$

$$\mathfrak{R}(\varsigma) = \left( \sqrt{-\frac{N}{T(2-m^2)}}\, dn\left( \sqrt{\frac{N}{2-m^2}} p\varsigma \right) \right)^{\frac{1}{p}}, \quad N > 0, \quad L = \frac{N^2 (1-m^2)}{T(2-m^2)^2}, \tag{2.10}$$

and

$$\mathfrak{R}(\varsigma) = \left( \sqrt{-\frac{Nm^2}{T(m^2+1)}}\, sn\left( \sqrt{-\frac{N}{m^2+1}} p\varsigma \right) \right)^{\frac{1}{p}}, \; N < 0, L = \frac{N^2 m^2}{T(m^2+1)^2}. \tag{2.11}$$

2.0.4. Case 4

If $L = M = T = 0$, substitute in Eq (2.2), we get bright soliton solution for Eq (1.1):

$$\mathfrak{R}(\varsigma) = \left( -\frac{N}{O} \operatorname{sech}^2 \left( \frac{\sqrt{N}}{2} p\varsigma \right) \right)^{\frac{1}{p}}, \; N > 0, \; O < 0, \tag{2.12}$$

a periodic solution:

$$\mathfrak{R}(\varsigma) = \left( -\frac{N}{O} \sec^2 \left( \frac{\sqrt{-N}}{2} p\varsigma \right) \right)^{\frac{1}{p}}, \; N < 0, \; O > 0, \tag{2.13}$$

and a rational solution:

$$\mathfrak{R}(\varsigma) = \left( \frac{4}{O(p\varsigma)^2} \right)^{\frac{1}{p}}, \; N = 0, \; O < 0. \tag{2.14}$$

2.0.5. Case 5

If $M = T = 0$, $O > 0$, substitute in Eq (2.2), we get Weierstrass elliptic function solution for Eq (1.1):

$$\mathfrak{R}(\varsigma) = \left( \chi\left( \frac{\sqrt{O}}{2} p\varsigma, q_2, q_3 \right) \right)^{\frac{1}{p}}, \tag{2.15}$$

where $q_2 = -\frac{4M}{D}$, $q_3 = -\frac{4L}{O}$.

2.0.6. Case 6

If $M = O = 0$, substitute in Eq (2.2), we get Weierstrass elliptic function solution for Eq (1.1):
**a**.

$$\mathfrak{R}(\varsigma) = \left(\frac{1}{T}\chi(p\varsigma, q_2, q_3) - \frac{N}{3}\right)^{\frac{1}{2p}}, \tag{2.16}$$

where $q_2 = \frac{4N^2-12LT}{3}$, $q_3 = \frac{4N(-2N^2+9LT)}{27}$,
**b**.

$$\mathfrak{R}(\varsigma) = \left(\frac{3L}{3\chi(p\varsigma, q_2, q_3) - N}\right)^{\frac{1}{2p}}, \tag{2.17}$$

where $q_2 = \frac{4N^2-12LT}{3}$, $q_3 = \frac{4N(-2N^2+9LT)}{27}$,
**c**.

$$\mathfrak{R}(\varsigma) = \left(\frac{\sqrt{12L\chi(p\varsigma, q_2, q_3) + 2L(2N+\pi)}}{12\chi(p\varsigma, q_2, q_3) + \pi}\right)^{\frac{1}{p}}, \tag{2.18}$$

where $q_2 = -\frac{1}{12}(5N\pi + 4N^2 + 33LNT)$, $q_3 = -\frac{4N}{216}(-21N^2\pi + 63LT\pi - 20N^3 + 27LNT)$
$and\pi = \frac{1}{2}(-5N \pm \sqrt{9N^2 - 36LT})$,
**d**.

$$\mathfrak{R}(\varsigma) = \left(\frac{6\sqrt{L}(\chi(p\varsigma, q_2, q_3) + N\sqrt{L})}{3\chi'(p\varsigma, q_2, q_3)}\right)^{\frac{1}{p}}, \tag{2.19}$$

where $\chi'(p\varsigma, q_2, q_3) = \frac{d\chi(p\varsigma, q_2, q_3)}{d\varsigma}$, $q_2 = \frac{N^2}{12} + LT$, $q_3 = \frac{LTN^3}{6}$,

**e**.

$$\mathfrak{R}(\varsigma) = \left(\frac{3\sqrt{T^{-1}}\chi'(p\varsigma, q_2, q_3)}{6\chi(p\varsigma, q_2, q_3) + N}\right)^{\frac{1}{p}}. \tag{2.20}$$

where $q_2 = \frac{N^2}{12} + LT$, $q_3 = \frac{LTN^3}{6}$.

2.0.7. Case 7

If $M = O = 0$, $L = \frac{5N^2}{36T}$, substitute in Eq (2.2), we get Weierstrass elliptic function solution for Eq (1.1):

$$\mathfrak{R}(\varsigma) = \left(\frac{N\sqrt{-\frac{15N}{2T}}\chi(p\varsigma, q_2, q_3)}{3\chi(p\varsigma, q_2, q_3) + N}\right)^{\frac{1}{p}}, \tag{2.21}$$

where $q_2 = \frac{2N^2}{9} + LT$, $q_3 = \frac{N^3}{54}$.

Here $q_2$ and $q_3$ are called invariants of the Weierstrass elliptic function.

2.0.8. Case 8

If $L = M = 0$, substitute in Eq (2.2), we get three positive soliton solutions for Eq (1.1):

$$\mathfrak{R}(\varsigma) = \left(\frac{1}{\cosh(\sqrt{N}p\varsigma) - \frac{O}{2N}}\right)^{\frac{1}{p}},\ N > 0,\ O < 2N,\ T = \frac{O^2}{4N} - N, \tag{2.22}$$

$$\mathfrak{R}(\varsigma) = \left(\frac{1}{2}\sqrt{\frac{N}{T}}\left(1 + \epsilon\tanh\left(\frac{1}{2}\sqrt{N}p\varsigma\right)\right)\right)^{\frac{1}{p}},\ N > 0,\ T > 0,\ O = -2\sqrt{NT}, \epsilon = \pm 1, \tag{2.23}$$

and

$$\mathfrak{R}(\varsigma) = \left(\frac{1}{(\frac{1}{2}p\varsigma)^2 - T}\right)^{\frac{1}{p}},\ N = 0,\ O = 1,\ T < 0. \tag{2.24}$$

2.0.9. Case 9

If $L = M = 0,\ N > 0$, substitute in Eq (2.2), we get hyperbolic function solutions for Eq (1.1):

$$\mathfrak{R}(\varsigma) = \left(\frac{2N\operatorname{sech}^2\left(\frac{\sqrt{N}}{2}p\varsigma\right)}{(\sqrt{O^2 - 4NT} - O)\operatorname{sech}^2\left(\frac{\sqrt{N}}{2}p\varsigma\right) - 2\sqrt{O^2 - 4NT}}\right)^{\frac{1}{p}},\ O^2 - 4NT > 0, \tag{2.25}$$

$$\mathfrak{R}(\varsigma) = \left(\frac{2N\operatorname{csch}^2\left(\frac{\sqrt{N}}{2}p\varsigma\right)}{(\sqrt{O^2 - 4NT} - O)\operatorname{csch}^2\left(\frac{\sqrt{N}}{2}p\varsigma\right) + 2\sqrt{O^2 - 4NT}}\right)^{\frac{1}{p}},\ O^2 - 4NT > 0. \tag{2.26}$$

2.0.10. Case 10

If $L = M = 0,\ N < 0$, substitute in Eq (2.2), we get periodic function solutions for Eq (1.1):

$$\mathfrak{R}(\varsigma) = \left(\frac{2N\sec^2\left(\frac{\sqrt{-N}}{2}p\varsigma\right)}{(\sqrt{O^2 - 4NT} - O)\sec^2\left(\frac{\sqrt{-N}}{2}p\varsigma\right) - 2\sqrt{O^2 - 4NT}}\right)^{\frac{1}{p}},\ O^2 - 4NT > 0, \tag{2.27}$$

$$\mathfrak{R}(\varsigma) = \left(\frac{2N\csc^2\left(\frac{\sqrt{-N}}{2}p\varsigma\right)}{(\sqrt{O^2 - 4NT} - O)\csc^2\left(\frac{\sqrt{-N}}{2}p\varsigma\right) - 2\sqrt{O^2 - 4NT}}\right)^{\frac{1}{p}},\ O^2 - 4NT > 0. \tag{2.28}$$

*2.1. Mathematical analysis*

Balancing $\varphi''$ and $\varphi^2$ in Eq (1.1) by using Eq (2.3), we get:

$$n + 2p = 2n \Longrightarrow n = 2p, \tag{2.29}$$

Now, Eq (1.1) has the formal solution:

$$\varphi(\varsigma) = \rho\mathfrak{R}^{2p}(\varsigma),\ \rho > 0, \tag{2.30}$$

Substituting Eq (2.30) along with Eq (2.2) into Eq (1.1), collecting all the coefficients of $\mathfrak{R}^{jp}(\varsigma)$, $(j = 0,\ 1\ 2,\ 3,\ 4)$, we get the following set of algebraic equations:

$$\begin{aligned}
\mathfrak{R}^{4p}(\varsigma) &: 6p^2Tv^2\rho - 6p^2T\eta^2\rho - \vartheta\rho^2 = 0,\\
\mathfrak{R}^{3p}(\varsigma) &: 25Op^2v^2\rho - 5Op^2\eta^2\rho = 0,\\
\mathfrak{R}^{2p}(\varsigma) &: 4Np^2v^2\rho - 4Np^2\eta^2\rho + \theta\rho = 0,\\
\mathfrak{R}^{p}(\varsigma) &: 3Mp^2v^2\rho - 3Mp^2\eta^2\rho = 0,\\
\mathfrak{R}^{0p}(\varsigma) &: -2Lp^2v^2\rho - 2Lp^2\eta^2\rho = 0.
\end{aligned} \tag{2.31}$$

With the aid of the solutions from Eqs (2.4)–Eq (2.28), here are the different types of solutions we have:

**Type 1a**.

In Case 1, $L = M = O = 0$, then we obtain the following results by resolving the algebraic Eq (2.31), above:

$$\begin{aligned}
N &= -\frac{\theta}{4P^2(v^2 - \eta^2)}\\
\rho &= \frac{6T(P^2v^2 - P^2\eta^2)}{\vartheta},
\end{aligned} \tag{2.32}$$

provided $N > 0,\quad T < 0$.

Substituting Eq (2.32) along with Eq (2.4) into Eq (2.30), we have the bright soliton solutions for NLKGM in the form:

$$\mathfrak{R}(x,t) = \frac{3\theta\sec\left(\frac{(-tv+x)\sqrt{\theta}}{2\sqrt{(v-\eta)(v+\eta)}}\right)}{\sqrt{\frac{\theta}{p^2T(v^2-\eta^2)}}\vartheta}. \tag{2.33}$$

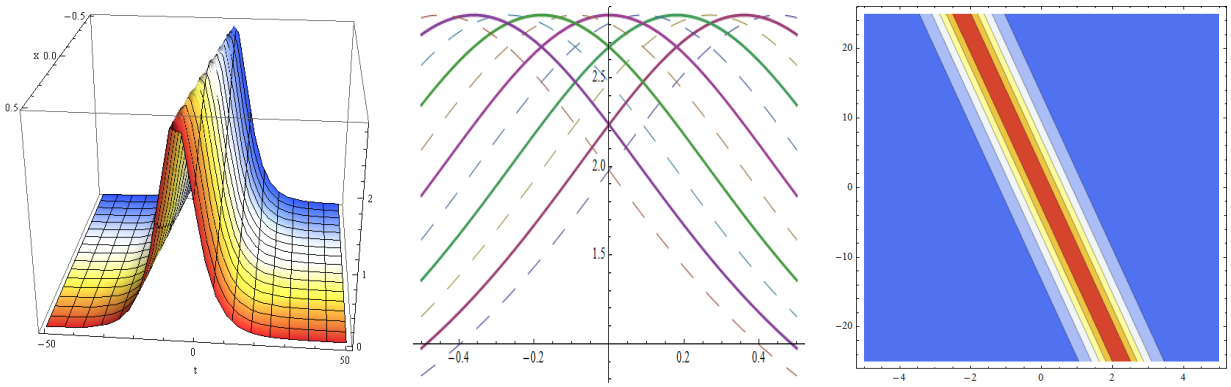

**(a)** **(b)** **(c)**

**Figure 1.** Bright soliton solution for the NLKGM equation within the interval $-0.5 \leqslant x \leqslant 0.5$ and $-50 \leqslant t \leqslant 50$.

**Type 1b**.

In Case 1, $L = M = O = 0$, then we obtain the following results by resolving the algebraic Eq (2.31), above:

$$N = -\frac{\theta}{4P^2(v^2 - \eta^2)} \tag{2.34}$$
$$\rho = \frac{6T(P^2v^2 - P^2\eta^2)}{\vartheta},$$

provided $N < 0, \quad T > 0$.

Substituting Eq (2.34) along with Eq (2.5) into Eq (2.30), we have the periodic soliton solutions for NLKGM in the form:

$$\Re(x,t) = \frac{3\theta \sec\left(\frac{1}{2}(-tv + x)\sqrt{\frac{\theta}{v^2-\eta^2}}\right)}{\sqrt{\frac{\theta}{p^2T(v^2-\eta^2)}}\vartheta}. \tag{2.35}$$

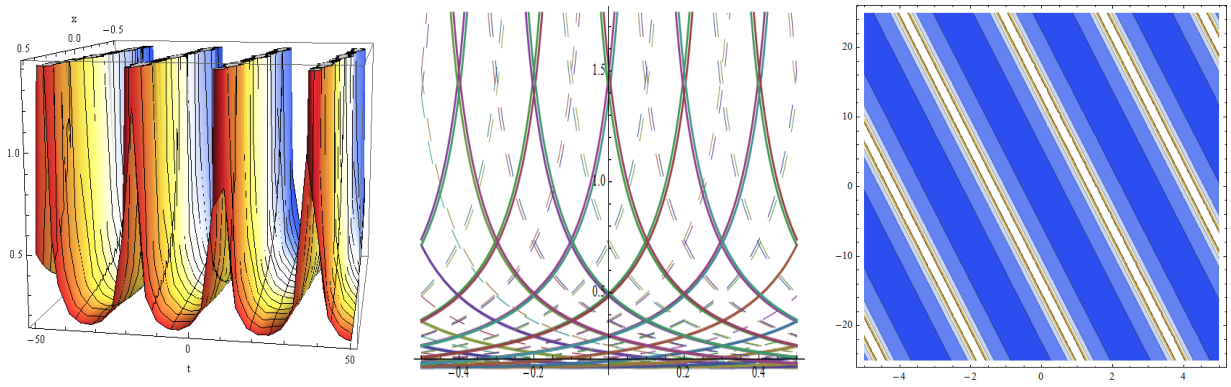

**(a)** **(b)** **(c)**

**Figure 2.** Periodic soliton solution for the NLKGM equation within the interval $-0.5 \leqslant x \leqslant 0.5$ and $-50 \leqslant t \leqslant 50$.

**Type 1c**.

In Case 1, $L = M = O = 0$, then we obtain the following results by resolving the algebraic Eq (2.31), above:

$$N = -\frac{\theta}{4P^2(v^2 - \eta^2)}$$
$$\rho = \frac{6T(P^2v^2 - P^2\eta^2)}{\vartheta}, \tag{2.36}$$

provided $N = 0, \quad T > 0, \quad \epsilon = \pm$.

Substituting Eq (2.36) along with Eq (2.6) into Eq (2.30), we have a rational soliton solutions for NLKGM in the form:

$$\Re(x,t) = \frac{6p\sqrt{T}(v^2 - \eta^2)\epsilon}{(tv - x)\vartheta}. \tag{2.37}$$

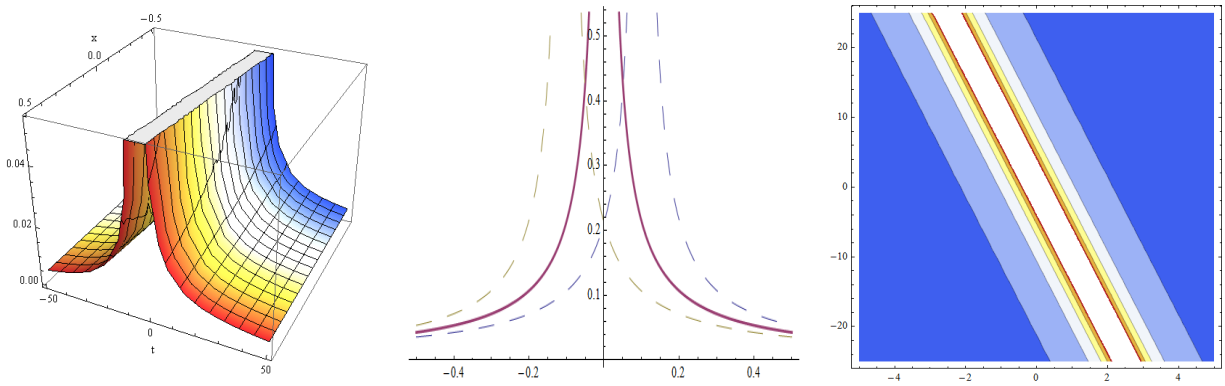

**(a)** **(b)** **(c)**

**Figure 3.** Rational soliton solution for the NLKGM equation within the interval $-0.5 \leqslant x \leqslant 0.5$ and $-50 \leqslant t \leqslant 50$.

**Type 2a**.

In Case 2, $M = O = 0, \ L = \frac{N^2}{4T}$, then we obtain the following results by resolving the algebraic Eq (2.31), above:

$$N = \frac{\theta}{8P^2\eta^2}$$
$$\rho = -\frac{12P^2T\eta^2}{\vartheta}, \tag{2.38}$$

provided $N > 0, \quad T < 0, \quad \epsilon = \pm 1$.

Substituting Eq (2.38) along with Eq (2.7) into Eq (2.30), we have dark soliton solutions for NLKGM in the form:

$$\Re(x,t) = \frac{3\sqrt{2}\theta\epsilon \tanh\left(\frac{p(-tv+x)\sqrt{\frac{\theta}{p^2\eta^2}}}{2\sqrt{2}}\right)}{\sqrt{-\frac{\theta}{p^2T\eta^2}}\vartheta}. \tag{2.39}$$

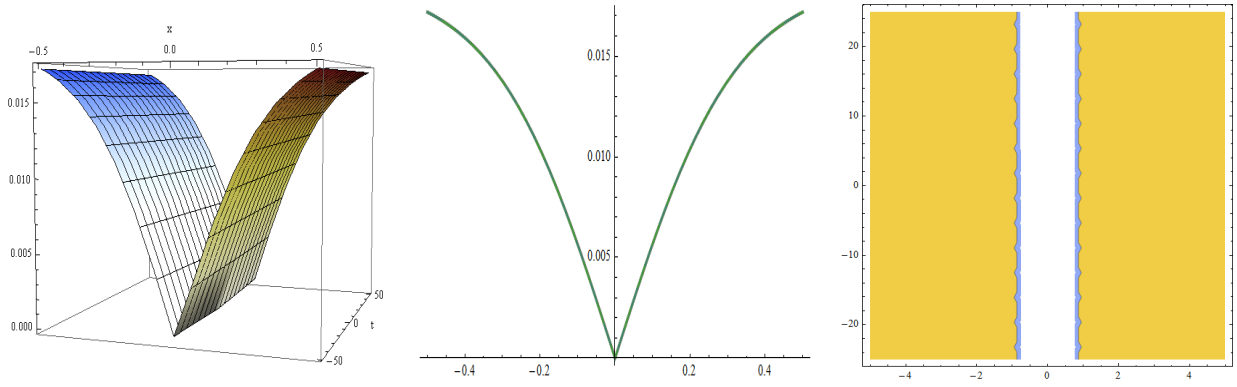

**(a)** **(b)** **(c)**

**Figure 4.** Dark soliton solution for the NLKGM equation within the interval $-0.5 \leqslant x \leqslant 0.5$ and $-50 \leqslant t \leqslant 50$.

**Type 2b**.

In Case 2, $M = O = 0,\ L = \frac{N^2}{4T}$, then we obtain the following results by resolving the algebraic Eq (2.31), above:

$$N = \frac{\theta}{8P^2\eta^2} \tag{2.40}$$
$$\rho = -\frac{12P^2T\eta^2}{\vartheta},$$

provided $N < 0,\ \ T > 0,\ \ \epsilon = \pm 1$.

Substituting Eq (2.40) along with Eq (2.8) into Eq (2.30), we have periodic soliton solutions for NLKGM in the form:

$$\Re(x,t) = \frac{3\sqrt{2}\theta\epsilon \tan\left(\frac{p(-tv+x)\sqrt{-\frac{\theta}{p^2\eta^2}}}{2\sqrt{2}}\right)}{\sqrt{-\frac{\theta}{p^2T\eta^2}}\vartheta}. \tag{2.41}$$

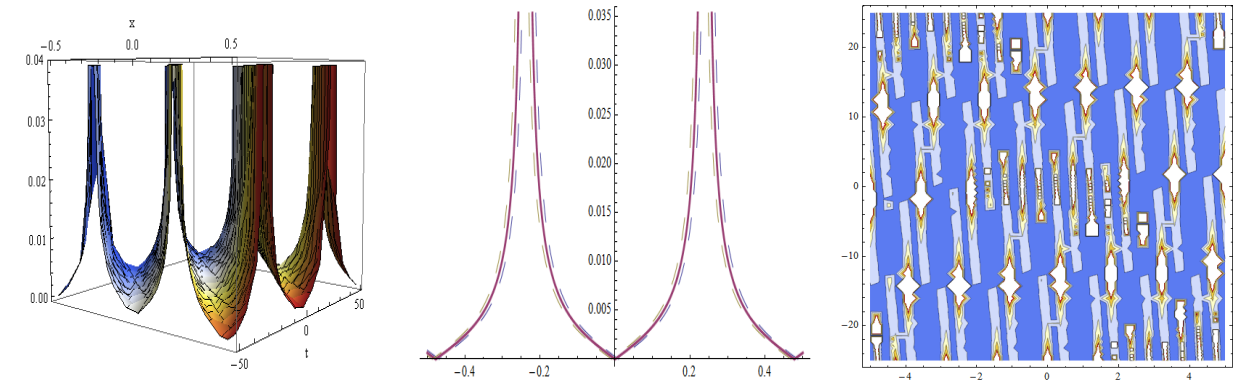

**(a)** **(b)** **(c)**

**Figure 5.** Periodic soliton solution for the NLKGM equation within the interval $-0.5 \leqslant x \leqslant 0.5$ and $-50 \leqslant t \leqslant 50$.

**Type 3**.

In Case 7, $M = O = 0,\ L = \frac{5N^2}{36T}$, then we obtain the following results by resolving the algebraic Eq (2.31), above:

$$N = -\frac{\theta}{8P^2v^2} \tag{2.42}$$
$$\rho = -\frac{12P^2T\eta^2}{\vartheta},$$

provided $q_2 = \frac{2N^2}{9} + LT,\ \ q_3 = \frac{N^3}{54}$.

Substituting Eq (2.42) along with Eq (2.21) into Eq (2.30), we have Weierstrass elliptic function solution for NLKGM as:

$$\Re(x,t) = \left(\frac{N\sqrt{\frac{-15N}{2T}(WeierstrassP(P\varsigma, q_2, q_3))}}{3WeierstrassP(P\varsigma, q_2, q_3) + N}\right). \tag{2.43}$$

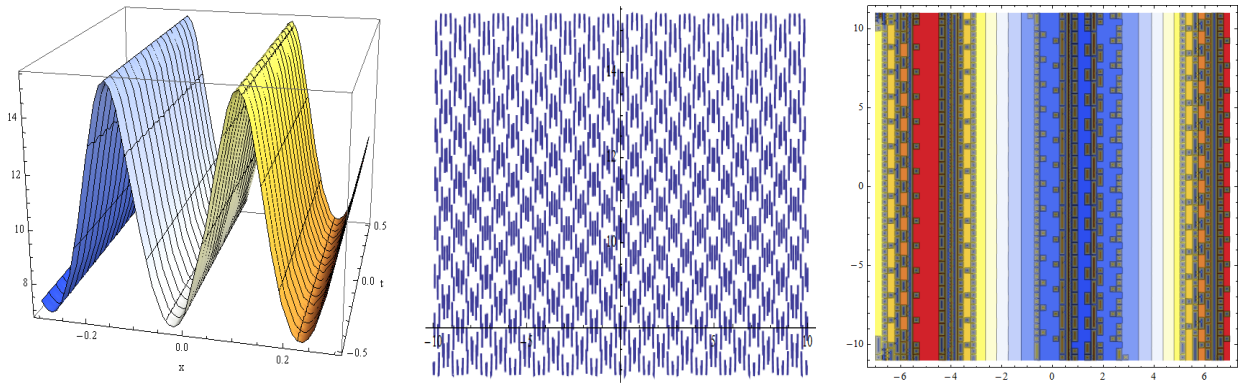

**(a)** **(b)** **(c)**

**Figure 6.** Weierstrass elliptic soliton solution for the NLKGM equation within the interval $-0.5 \leqslant x \leqslant 0.5$ and $-50 \leqslant t \leqslant 50$.

**Type 4**.

In Case 8, $L = M = 0,\ T = \frac{O^2}{4N} - N$, then we obtain the following results by resolving the algebraic Eq (2.31), above:

$$N = -\frac{\theta}{4P^2(v^2 - \eta^2)} \tag{2.44}$$
$$\rho = -\frac{3\theta}{2\vartheta},$$

provided $N > 0,\ \ O < 2N$.

Substituting Eq (2.44) along with Eq (2.22) into Eq (2.30), we have positive solutions for NLKGM in the form:

$$\Re(x,t) = \frac{3\theta \sec\left(\frac{(-tv+x)\sqrt{\theta}}{2\sqrt{(v-\eta)(v+\eta)}}\right)}{2\vartheta}. \tag{2.45}$$

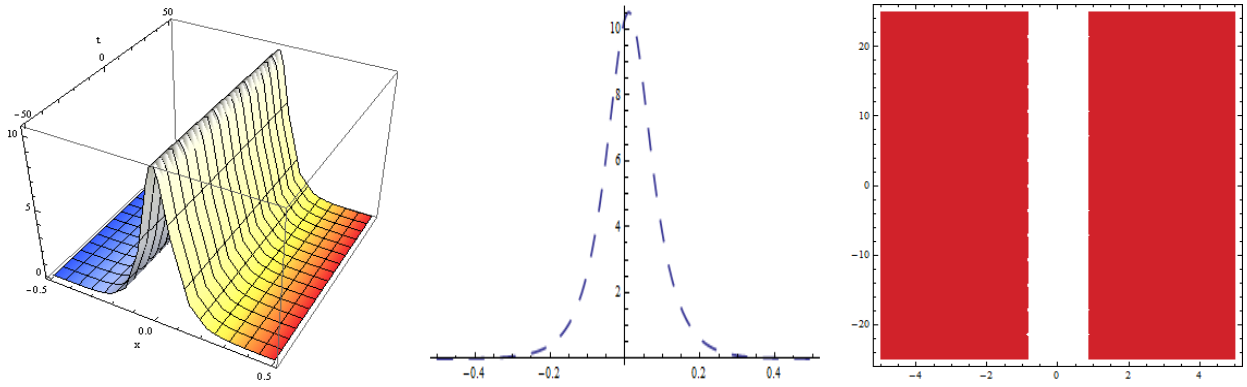

(a) (b) (c)

**Figure 7.** Positive soliton solution for the NLKGM equation within the interval $-0.5 \leqslant x \leqslant 0.5$ and $-50 \leqslant t \leqslant 50$.

**Type 5a**.

In Case 9, $L = M = 0,\ N > 0$, then we obtain the following results by resolving the algebraic Eq (2.31), above:

$$N = -\frac{\theta}{4P^2(v^2 - \eta^2)} \qquad (2.46)$$
$$\rho = \frac{6T(P^2v^2 - P^2\eta^2)}{\vartheta},$$

provided $O^2 - 4NT > 0$.

Substituting Eq (2.46) along with Eq (2.25) into Eq (2.30), we have the hyperbolic function solutions for NLKGM in the form:

$$\Re(x,t) = \frac{3T\theta \sec\left(\frac{(-tv+x)\sqrt{\theta}}{2\sqrt{(v-\eta)(v+\eta)}}\right)}{2\sqrt{-nT\vartheta}}. \qquad (2.47)$$

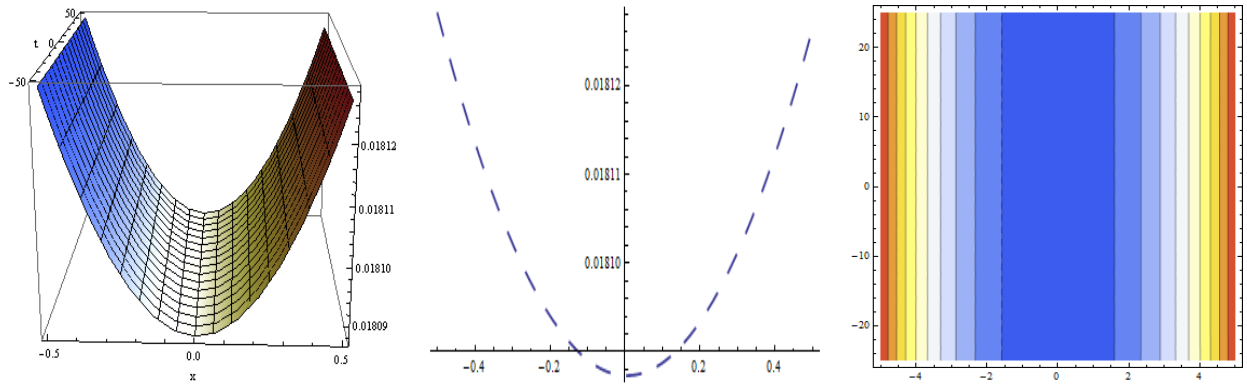

(a) (b) (c)

**Figure 8.** Hyperbolic soliton solution for the NLKGM equation within the interval $-0.5 \leqslant x \leqslant 0.5$ and $-50 \leqslant t \leqslant 50$.

**Type 5b**.

In Case 9, $L = M = 0$, $N > 0$, then we obtain the following results by resolving the algebraic Eq (2.31), above:

$$N = -\frac{\theta}{4P^2(v^2 - \eta^2)}$$
$$\rho = \frac{6T(P^2v^2 - P^2\eta^2)}{\vartheta}, \tag{2.48}$$

provided $O^2 - 4NT > 0$.

Substituting Eq (2.48) along with Eq (2.26) into Eq (2.30), we have the hyperbolic function solutions for NLKGM in the form:

$$\Re(x,t) = \frac{3T\theta \sec\left(\frac{(-tv+x)\sqrt{\theta}}{2\sqrt{(v-\eta)(v+\eta)}}\right)}{2\sqrt{-nT}\vartheta}. \tag{2.49}$$

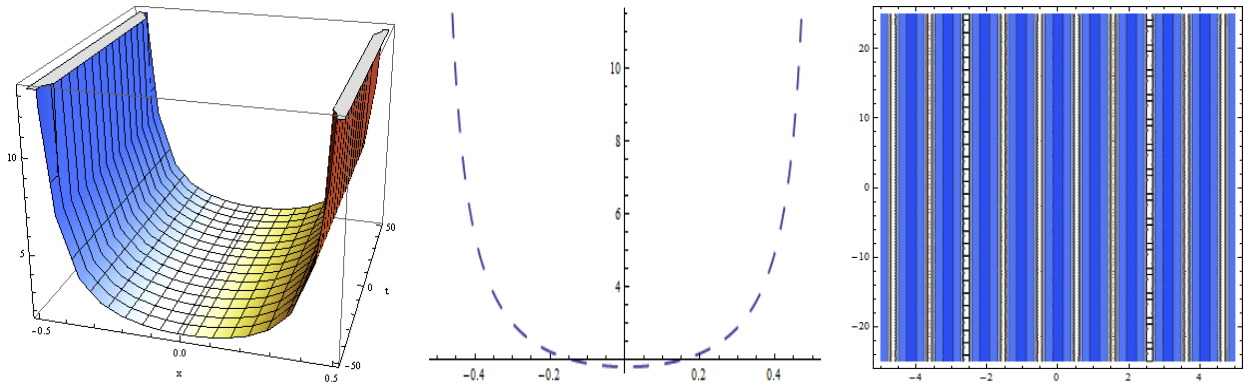

**(a)** **(b)** **(c)**

**Figure 9.** Hyperbolic soliton solution for the NLKGM equation within the interval $-0.5 \leqslant x \leqslant 0.5$ and $-50 \leqslant t \leqslant 50$.

**Type 6a**.

In Case 10, $L = M = 0$, $N < 0$, then we obtain the following results by resolving the algebraic Eq (2.31), above:

$$N = -\frac{\theta}{4P^2(v^2 - \eta^2)}$$
$$\rho = \frac{6T(P^2v^2 - P^2\eta^2)}{\vartheta}, \tag{2.50}$$

provided $O^2 - 4NT > 0$.

Substituting Eq (2.50) along with Eq (2.27) into Eq (2.30), we have the periodic function solutions for NLKGM in the form:

$$\Re(x,t) = \frac{3T\theta}{O\vartheta + \sqrt{-4NT + O^2}\vartheta \cos\left(\frac{1}{2}(-tv + x)\sqrt{\frac{\theta}{v^2-\eta^2}}\right)}. \tag{2.51}$$

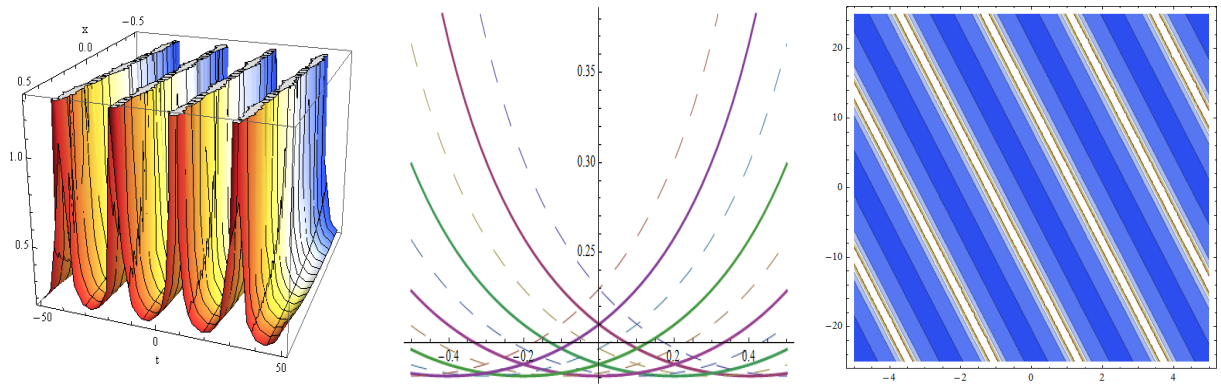

(a) (b) (c)

**Figure 10.** Periodic soliton solution for the NLKGM equation within the interval $-0.5 \leqslant x \leqslant 0.5$ and $-50 \leqslant t \leqslant 50$.

**Type 6b**.

In Case 10, $L = M = 0$, $N < 0$, then we obtain the following results by resolving the algebraic Eq (2.31), above:

$$N = -\frac{\theta}{4P^2(v^2 - \eta^2)} \tag{2.52}$$
$$\rho = \frac{6T(P^2v^2 - P^2\eta^2)}{\vartheta},$$

provided $O^2 - 4NT > 0$.

Substituting Eq (2.52) along with Eq (2.28) into Eq (2.30), we have the periodic function solutions for NLKGM in the form:

$$\Re(x,t) = \frac{3T\theta}{O\vartheta - \sqrt{-4NT + O^2}\vartheta \cos\left(\frac{1}{2}(-tv + x)\sqrt{\frac{\theta}{v^2-\eta^2}}\right)}. \tag{2.53}$$

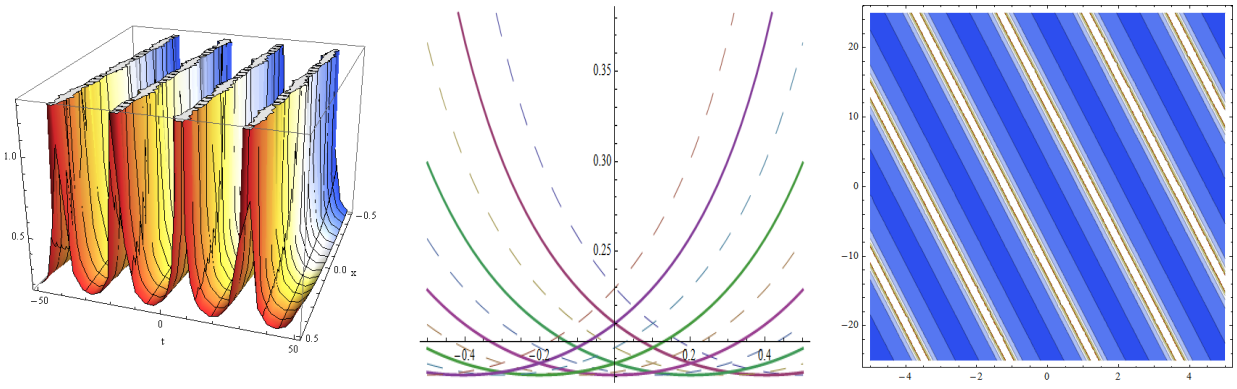

(a) (b) (c)

**Figure 11.** Periodic soliton solution for the NLKGM equation within the interval $-0.5 \leqslant x \leqslant 0.5$ and $-50 \leqslant t \leqslant 50$.

Now in this section, using the finite difference scheme, we will examine the governing model for numerical solutions utilizing a combination of forward, backward, and centered difference schemes:

## 3. Finite difference scheme (FDS)

The Forward-forward difference scheme (F-FDS), Forward-backward difference scheme (F-BDS), Forward-centered difference scheme (F-CDS), Backward-backward difference scheme (B-BDS), Forward-forward difference scheme (B-FDS), Backward-centered difference scheme (B-CDS), Centered-centered difference scheme (C-CDS), Centered-forward difference scheme (C-FDS), Centered-backward difference scheme (C-BDS) and Backward-forward difference scheme (B-FDS) will be used to study FDS in this section.

We know the Tayler's series expansion,

$$\omega(x+\ell) = \omega(x) + \ell\omega'(x) + \frac{\ell^2\omega''(x)}{2!} + ..., \tag{3.1}$$

First Derivative Approximation,

$$\omega'(x) \approx \frac{\omega(x+\ell) - \omega(x)}{\ell}, \tag{3.2}$$

Similarly, Second Derivative Approximation,

$$\omega''(x) \approx \frac{\omega(x+\ell) - 2\omega(x) + \omega(x-\ell)}{\ell^2}. \tag{3.3}$$

### *3.1. F-FDS*

A numerical technique used to estimate a function's derivative at a specific point is called the F-FDS. It uses a finite difference method in which two closely spaced locations are chosen, one slightly ahead of the other and the difference in function values between them is computed. This method produces an approximation of the derivative of the function at the chosen place, which makes it particularly useful for such numerical approximations.

From Tayler's series expansion, we get,

$$\wp_x \approx \frac{\wp(x+\ell,t) - \wp(x,t)}{\ell_x}, \tag{3.4}$$

$$\wp_{xx} \approx \frac{\wp(x+\ell,t) - 2\wp(x,t) - \wp(x-\ell,t)}{\ell_x^2}, \tag{3.5}$$

$$\wp_t \approx \frac{\wp(x,t+\hbar) - \wp(x,t)}{\ell_t}, \tag{3.6}$$

$$\wp_{tt} \approx \frac{\wp(x,t+\hbar) - 2\wp(x,t) + \wp(x,t-\hbar)}{\ell_t^2}. \tag{3.7}$$

Substitute Eqs (3.4)–Eq (3.7) into Eq (1.1), we get,

$$\wp_{i,j_+1} = \frac{\alpha^2\ell_t^2(\wp_{i+1,j} - 2\wp_{i,j} - \wp_{i-1,j})}{\ell_x^2} - \ell_t^2\beta(\wp_{i,j}) + \ell_t^2\gamma(\wp_{i,j})^2 + 2\wp_{i,j} - \wp_{i,j_{-1}}, \tag{3.8}$$

let

$$\gamma_1 = \frac{\alpha^2\ell_t^2}{\ell_x^2}, \gamma_2 = \ell_t^2\beta, \gamma_3 = \ell_t^2\gamma, \tag{3.9}$$

$$\wp_{i,j_+1} = \gamma_1(\wp_{i+1,j}) + (2\gamma_1 + 2 - \gamma_2)\wp_{i,j} - \gamma_1(\wp_{i+1,j}) - (\wp_{i,j_{-1}}) + \gamma_3(\wp_{i,j})^2. \tag{3.10}$$

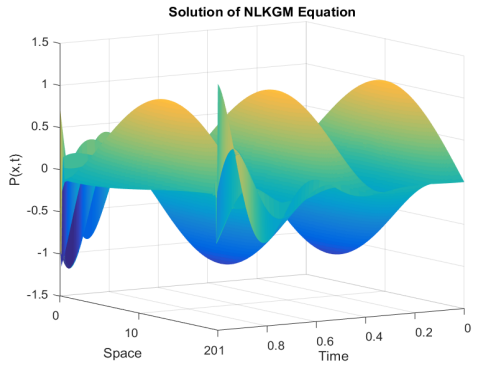


**(a)**

**Figure 12.** F-FDS.

### *3.2. F-BDS*

The backward difference method approximates derivatives using a data point that is slightly behind the reference point. Differential equation solutions can, however, be estimated numerically using the F-BDS method. By integrating components of the forward and backward difference schemes, this method produces the three basic types of finite difference schemes.

From Tayler's series expansion, we get,

$$\wp_{tt} \approx \frac{\wp(x, t+\hbar) - 2\wp(x,t) + \wp(x, t-\hbar)}{\ell_t^2}, \tag{3.11}$$

$$\wp_{xx} \approx \frac{\wp(x-2\ell, t) - 2\wp(x-\ell, t) + \wp(x,t)}{\ell_x^2}. \tag{3.12}$$

Substitute Eqs (3.11) and (3.12) into Eq (1.1), we get,

$$\wp_{i,j_+1} = \frac{\alpha^2\ell_t^2(\wp_{i-2,j} - 2\wp_{i-1,j} + \wp_{i,j})}{\ell_x^2} - \ell_t^2\beta(\wp_{i,j}) + \ell_t^2\gamma(\wp_{i,j})^2 + 2\wp_{i,j} - \wp_{i,j_{-1}}, \tag{3.13}$$

let

$$\gamma_1 = \frac{\alpha^2\ell_t^2}{\ell_x^2}, \gamma_2 = \ell_t^2\beta, \gamma_3 = \ell_t^2\gamma, \tag{3.14}$$

$$\wp_{i,j_+1} = \gamma_1(\wp_{i-2,j}) - 2\gamma_1(\wp_{i-1,j}) - (\wp_{i,j-1}) + (\gamma_1 + 2 - \gamma_2)\wp_{i,j} + \gamma_3(\wp_{i,j})^2. \tag{3.15}$$

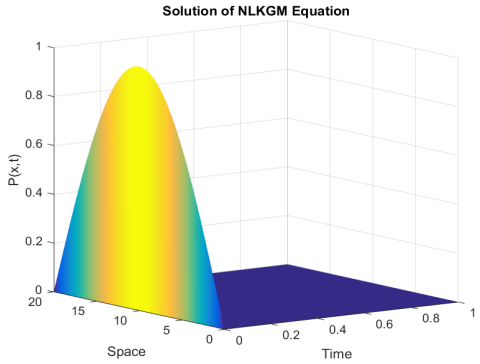


**(a)**

**Figure 13.** F-BDS.

### *3.3. F-CDS*

By estimating the derivative more precisely, the centered difference approach improves accuracy by using data points in front of and behind the reference point. In order to provide a more precise approximation of the derivative, the F-CDS also contains two data points that are ahead of and two data points that are behind the reference point.

From Tayler's series expansion, we get,

$$\wp_{tt} \approx \frac{\wp(x, t+\hbar) - 2\wp(x,t) + \wp(x, t-\hbar)}{\ell_t^2}, \tag{3.16}$$

$$\wp_{xx} \approx \frac{\wp(x+\ell, t) - 2\wp(x,t) + \wp(x-\ell, t)}{\ell_x^2}. \tag{3.17}$$

Substitute Eqs (3.16) and (3.17) into Eq (1.1), we get,

$$\wp_{i,j_+1} = \frac{\alpha^2\ell_t^2(\wp_{i+1,j} - 2\wp_{i,j} + \wp_{i-1,j})}{\ell_x^2} - \ell_t^2\beta(\wp_{i,j}) + \ell_t^2\gamma(\wp_{i,j})^2 + 2\wp_{i,j} - \wp_{i,j_-1}, \tag{3.18}$$

let

$$\gamma_1 = \frac{\alpha^2\ell_t^2}{\ell_x^2}, \gamma_2 = \ell_t^2\beta, \gamma_3 = \ell_t^2\gamma, \tag{3.19}$$

$$\wp_{i,j_+1} = \gamma_1(\wp_{i+1,j}) + \gamma_1(\wp_{i-1,j}) + (2 - 2\gamma_1 - \gamma_2)\wp_{i,j} - \wp_{i,j_-1} + \gamma_3(\wp_{i,j})^2. \tag{3.20}$$

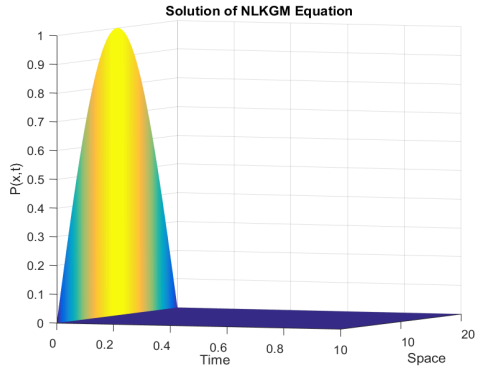


**(a)**

**Figure 14.** F-CDS.

.

### *3.4. B-BDS*

With an observation close to the point of interest, the "backward difference scheme" generates derivatives. The primary objective is to approximate the function's slope using solely historical data, paying close attention to historical data while it is being estimated.

From Tayler's series expansion, we get,

$$\wp_{xx} \approx \frac{\wp(x-2\ell,t)-2\wp(x-\ell,t)+\wp(x,t)}{\ell_x^2}, \tag{3.21}$$

$$\wp_{tt} \approx \frac{\wp(x,t)-2\wp(x,t-\hbar)+\wp(x,t-2\hbar)}{\ell_t^2}. \tag{3.22}$$

Substitute Eqs (3.21) and (3.22) into Eq (1.1), we get,

$$\wp_{i,j-2} = \frac{\alpha^2\ell_t^2(\wp_{i-2,j}-2\wp_{i-1,j}+\wp_{i,j})}{\ell_x^2} - \ell_t^2\beta(\wp_{i,j}) + \ell_t^2\gamma(\wp_{i,j})^2 + 2\wp_{i,j-1}-\wp_{i,j-2}, \tag{3.23}$$

let

$$\gamma_1 = \frac{\alpha^2\ell_t^2}{\ell_x^2}, \gamma_2 = \ell_t^2\beta, \gamma_3 = \ell_t^2\gamma, \tag{3.24}$$

$$\wp_{i,j-2} = \gamma_1(\wp_{i-2,j}) - 2\gamma_1(\wp_{i-1,j}) + (\gamma_1-\gamma_2-1)\wp_{i,j} + 2\wp_{i,j-1} + \gamma_3(\wp_{i,j})^2. \tag{3.25}$$

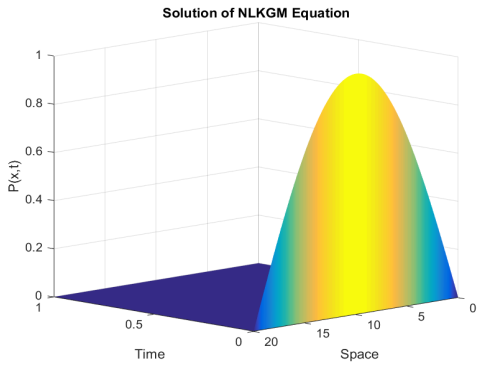


**(a)**

**Figure 15.** B-BDS.

### *3.5. B-FDS*

A method for numerically calculating a function's second derivative at a specific position is called the B-FDS. To achieve this and produce a more precise and well-rounded estimate of the second derivative, it skillfully integrates elements from both forward and backward difference schemes, utilizing information from both past and future areas.

From Tayler's series expansion, we get,

$$\wp_{tt} \approx \frac{\wp(x,t) - 2\wp(x,t-\hbar) + \wp(x,t-2\hbar)}{\ell_t^2}, \tag{3.26}$$

$$\wp_{xx} \approx \frac{\wp(x+\ell,t) - 2\wp(x,t) - \wp(x-\ell,t)}{\ell_x^2}. \tag{3.27}$$

Substitute Eqs (3.26) and (3.27) into Eq (1.1), we get,

$$\wp_{i,j\_2} = \frac{\alpha^2\ell_t^2(\wp_{i+1,j} - 2\wp_{i,j} - \wp_{i-1,j})}{\ell_x^2} - \ell_t^2\beta(\wp_{i,j}) + \ell_t^2\gamma(\wp_{i,j})^2 + 2\wp_{i,j-1} + \wp_{i,j\_2}, \tag{3.28}$$

let

$$\gamma_1 = \frac{\alpha^2\ell_t^2}{\ell_x^2}, \gamma_2 = \ell_t^2\beta, \gamma_3 = \ell_t^2\gamma, \tag{3.29}$$

$$\wp_{i,j\_2} = \gamma_1(\wp_{i+1,j}) - \gamma_1(\wp_{i-1,j}) + (-2\gamma_1 - 1 - \gamma_2)\wp_{i,j} + 2\wp_{i,j-1} + \gamma_3(\wp_{i,j})^2. \tag{3.30}$$

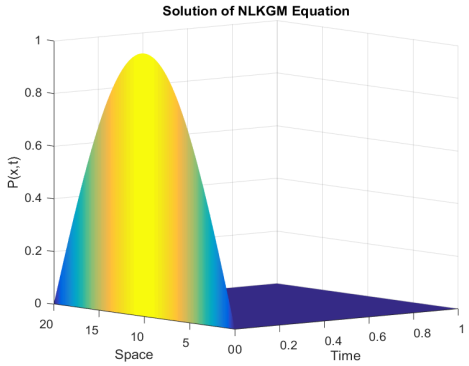


**(a)**

**Figure 16.** B-FDS.

### *3.6. B-CDS*

When data and historical data are present on both sides of the point of interest, the B-CDS is most useful for calculating the second derivative. This method works best when symmetric and historical data are available.

From Tayler's series expansion, we get,

$$\wp_{tt} \approx \frac{\wp(x,t) - 2\wp(x,t-\hbar) + \wp(x,t-2\hbar)}{\ell_t^2}, \tag{3.31}$$

$$\wp_{xx} \approx \frac{\wp(x+\ell,t) - 2\wp(x,t) + \wp(x-\ell,t)}{\ell_x^2}. \tag{3.32}$$

Substitute Eqs (3.31) and (3.32) into Eq (1.1), we get,

$$\wp_{i,j-2} = \frac{\alpha^2\ell_t^2(\wp_{i+1,j} - 2\wp_{i,j} - \wp_{i-1,j})}{\ell_x^2} - \ell_t^2\beta(\wp_{i,j}) + \ell_t^2\gamma(\wp_{i,j})^2 + 2\wp_{i,j-1} + \wp_{i,j-2}, \tag{3.33}$$

let

$$\gamma_1 = \frac{\alpha^2\ell_t^2}{\ell_x^2}, \gamma_2 = \ell_t^2\beta, \gamma_3 = \ell_t^2\gamma, \tag{3.34}$$

$$\wp_{i,j-2} = \gamma_1(\wp_{i+1,j}) + \gamma_1(\wp_{i-1,j}) + 2\wp_{i,j-1} + (-2\gamma_1 - 1 - \gamma_2)\wp_{i,j} + \gamma_3(\wp_{i,j})^2. \tag{3.35}$$

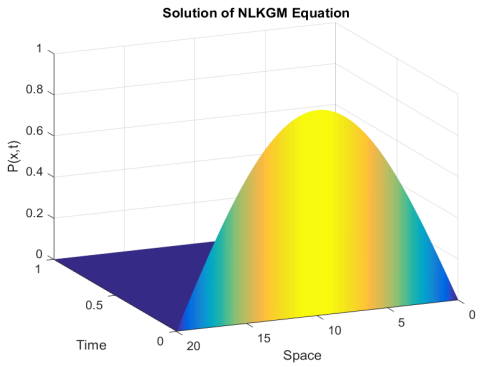


**(a)**

**Figure 17.** B-CDS.

### *3.7. C-CDS*

The "centered difference scheme" is a widely used numerical method for calculating derivatives at a given place, which makes use of data points from both the forward and backward directions relative to the point of interest.

From Tayler's series expansion, we get,

$$\wp_{xx} \approx \frac{\wp(x+\ell,t) - 2\wp(x,t) + \wp(x-\ell,t)}{\ell_x^2}, \tag{3.36}$$

$$\wp_{tt} \approx \frac{\wp(x,t+\hbar) - 2\wp(x,t) + \wp(x,t-\hbar)}{\ell_t^2}. \tag{3.37}$$

Substitute Eqs (3.36) and (3.37) into Eq (1.1), we get,

$$\wp_{i,j_+1} = \frac{\alpha^2\ell_t^2(\wp_{i+1,j} - 2\wp_{i,j} - \wp_{i-1,j})}{\ell_x^2} - \ell_t^2\beta(\wp_{i,j}) + \ell_t^2\gamma(\wp_{i,j})^2 + 2\wp_{i,j} + \wp_{i,j_-1}. \tag{3.38}$$

let

$$\gamma_1 = \frac{\alpha^2\ell_t^2}{\ell_x^2}, \gamma_2 = \ell_t^2\beta, \gamma_3 = \ell_t^2\gamma, \tag{3.39}$$

$$\wp_{i,j_+1} = \gamma_1(\wp_{i+1,j}) + (2 - 2\gamma_1 - \gamma_2)\wp_{i,j} + \gamma_1(\wp_{i-1,j}) - \wp_{i,j_-1} + \gamma_3(\wp_{i,j})^2. \tag{3.40}$$

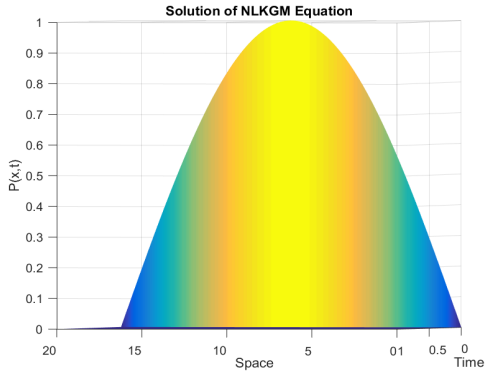


**(a)**

**Figure 18.** C-CDS.

### *3.8. C-FDS*

The C-FDS or combination of the forward and centered difference schemes, yields a more accurate derivative estimate. When working with data that is available with respect to a given time in the past as well as the future, this method performs well.

From Tayler's series expansion, we get,

$$\wp_{tt} \approx \frac{\wp(x, t+\hbar) - 2\wp(x,t) + \wp(x, t-\hbar)}{\ell_t^2}, \tag{3.41}$$

$$\wp_{xx} \approx \frac{\wp(x+\ell, t) - 2\wp(x,t) - \wp(x-\ell, t)}{\ell_x^2}. \tag{3.42}$$

Substitute Eqs (3.41) and (3.42) into Eq (1.1), we get,

$$\wp_{i,j_+1} = \frac{\alpha^2\ell_t^2(\wp_{i+1,j} - 2\wp_{i,j} - \wp_{i-1,j})}{\ell_x^2} - \ell_t^2\beta(\wp_{i,j}) + \ell_t^2\gamma(\wp_{i,j})^2 + 2\wp_{i,j} - \wp_{i,j_{-1}}, \tag{3.43}$$

let

$$\gamma_1 = \frac{\alpha^2\ell_t^2}{\ell_x^2}, \gamma_2 = \ell_t^2\beta, \gamma_3 = \ell_t^2\gamma, \tag{3.44}$$

$$\wp_{i,j_+1} = \gamma_1(\wp_{i+1,j}) - \gamma_1(\wp_{i-1,j}) - \wp_{i,j_{-1}} + (2 - 2\gamma_1 - \gamma_2)\wp_{i,j} + \gamma_3(\wp_{i,j})^2. \tag{3.45}$$

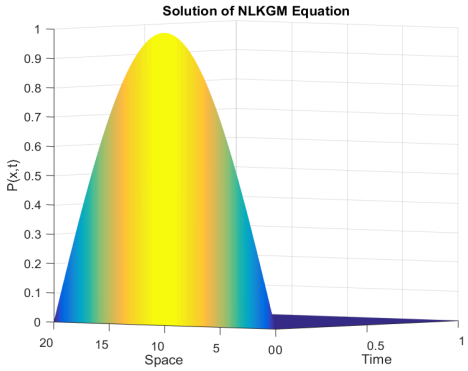


**(a)**

**Figure 19.** C-FDS.

### *3.9. C-BDS*

With the use of data points from the past and from both sides of the given position, the C-BDS seeks to estimate the derivative with accuracy and efficiency. This method improves accuracy by taking into account data from several angles close to the point of interest.

From Tayler's series expansion, we get,

$$\wp_{tt} \approx \frac{\wp(x, t+\hbar) - 2\wp(x,t) + \wp(x, t-\hbar)}{\ell_t^2}, \tag{3.46}$$

$$\wp_{xx} \approx \frac{\wp(x-2\ell, t) - 2\wp(x-\ell, t) + \wp(x,t)}{\ell_x^2}. \tag{3.47}$$

Substitute Eqs (3.46) and (3.47) into Eq (1.1), we get,

$$\wp_{i,j_+1} = \frac{\alpha^2\ell_t^2(\wp_{i-2,j} - 2\wp_{i-1,j} + \wp_{i,j})}{\ell_x^2} - \ell_t^2\beta(\wp_{i,j}) + \ell_t^2\gamma(\wp_{i,j})^2 + 2\wp_{i,j} + \wp_{i,j_-1}, \tag{3.48}$$

let

$$\gamma_1 = \frac{\alpha^2\ell_t^2}{\ell_x^2}, \gamma_2 = \ell_t^2\beta, \gamma_3 = \ell_t^2\gamma, \tag{3.49}$$

$$\wp_{i,j_+1} = \gamma_1(\wp_{i-2,j}) - 2\gamma_1(\wp_{i-1,j}) - \wp_{i,j_-1} + (\gamma_1 + 2 - \gamma_2)\wp_{i,j} + \gamma_3(\wp_{i,j})^2. \tag{3.50}$$

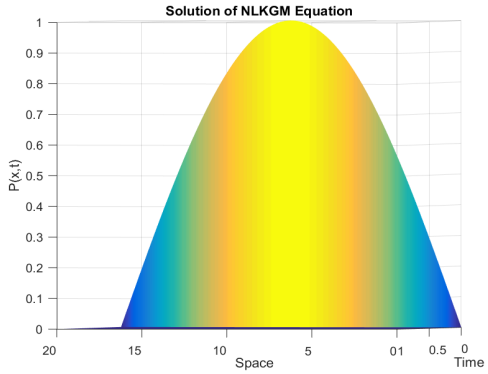


**(a)**

**Figure 20.** C-BDS.

**Table 1.** Comparison all of the approximate solutions $\wp_1(x,t)$, $\wp_2(x,t)$, $\wp_3(x,t)$.

| $\wp_1(x,t)$ | $\wp_2(x,t)$ | $\wp_3(x,t)$ |
|---|---|---|
| 0.0157 | 0.0156 | 0.0150 |
| 0.0314 | 0.0313 | 0.0304 |
| 0.0471 | 0.0470 | 0.0458 |
| 0.0627 | 0.0626 | 0.0611 |
| 0.0784 | 0.0783 | 0.0765 |
| 0.0941 | 0.0939 | 0.0918 |
| 0.1097 | 0.1095 | 0.1071 |
| 0.1253 | 0.1251 | 0.1224 |
| 0.1409 | 0.1406 | 0.1376 |
| 0.1564 | 0.1561 | 0.1529 |

This section will use the Lagrangian approach to approximate the NLKGM solution in order to find the Euler-lagrange equation, discrete lagrangian, and discrete Euler-lagrange equation:

## 4. Lagrangian approach

The Lagrangian for NLKGM is

$$L = \frac{1}{2}\wp_t^2 - \frac{1}{2}\alpha^2\wp_x^2 + \frac{1}{2}\beta\wp^2 - \frac{1}{3}\gamma\wp^3, \tag{4.1}$$

where

$$K.E = \frac{1}{2}\wp_t^2, \tag{4.2}$$

where K.E is the kinetic energy of NLKGM.

$$P.E = \frac{1}{2}\alpha^2\wp_x^2 + \frac{1}{2}\beta\wp^2 - \frac{1}{3}\gamma\wp^3. \tag{4.3}$$

where P.E is the potential energy of NLKGM.

The Euler-Lagrange equation in continuous form is provided by:

$$\frac{\partial L}{\partial \wp} + \frac{d}{dt}\left(\frac{\partial L}{\partial \wp_t}\right) - \frac{d}{dt}\left(\frac{\partial L}{\partial \wp_X}\right) = 0. \tag{4.4}$$

The Lagrangian density will now be discretized. With $\triangle_x$ and $\triangle_t$, respectively, representing the grid spacing of a uniform grid in both space and time, we can apply finite differences:

$$\frac{\partial L}{\partial \wp_t} = \wp_t, \tag{4.5}$$

$$\frac{\partial L}{\partial \wp_x} = \left(\frac{\wp_{i+1} - 2\wp_i + \wp_{i-1}}{\triangle_x^2}\right), \tag{4.6}$$

$$\frac{\partial L}{\partial \wp} = -\beta + \gamma \wp^2. \tag{4.7}$$

Now, substitute Eqs (4.5)–Eq (4.7) into Eq (4.4):

$$\frac{\partial \wp_t}{\partial t} + \frac{d}{dt}\left(\frac{\wp_{i+1} - 2\wp_i + \wp_{i-1}}{\triangle_x}\right) + \left(-\beta + \gamma \wp_i^2\right) = 0, \tag{4.8}$$

Apply finite differences to the time derivative:

$$\frac{\wp_t^{n+1} - \wp_t^n}{\triangle_t} - \frac{\wp_{i+1}^n - 2\wp_i^n + \wp_{i-1}^n}{\triangle_x^2} + \left(-\beta + \gamma(\wp_i^n)^2\right) = 0. \tag{4.9}$$

Solving this equation for $\wp_t^{n+1}$, we get,

$$\wp_t^{n+1} = \wp_t^n + \triangle_t\left(\frac{\wp_{i+1}^n - 2\wp_i^n + \wp_{i-1}^n}{\triangle_x^2} + (-\beta + \gamma(\wp_i^n)^2)\right). \tag{4.10}$$

For the NLKGM, this is the discrete Euler-Lagrange equation. In terms of values at the current time step and spatial coordinates, it represents the update strategy for the temporal derivative $\wp_t$ at the subsequent time step.

We are going to now analyze how analytical and numerical graphs compare. This shows that the error is minimum.

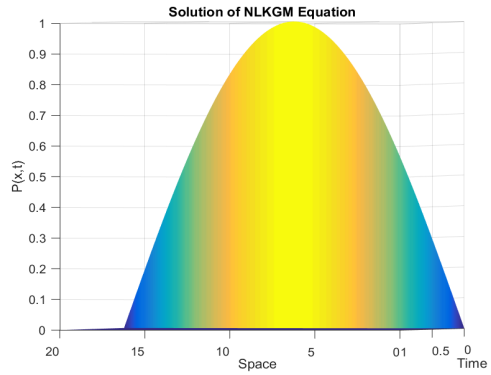


**(a)**

**Figure 21.** Analytical Graph.

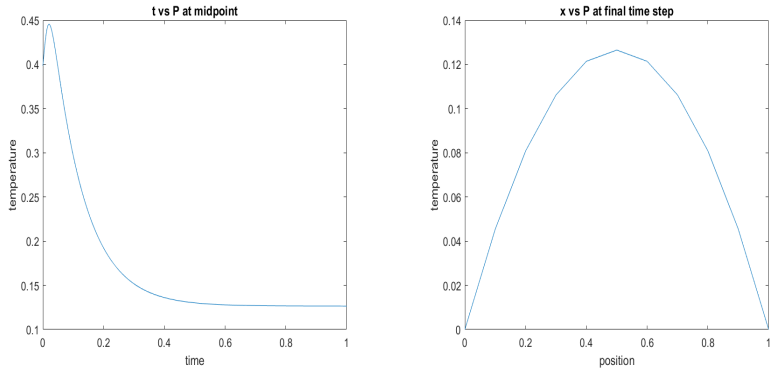


**(a)** **(b)**

**Figure 22.** Numerical Graph.

After compare both the graphs for the solutions of our governing model. we get "Relative Energy error graph" with the aid of this relative error formula:
$Error = abs(\frac{(H_e - H_n)}{H_e})$ :

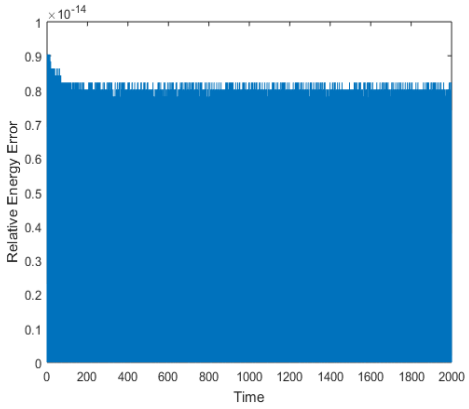


**(a)**

**Figure 23.** Relative energy error graph.

## 5. Results and discussion

In order to examine neutral scalar mesons linked with conserved scalar nucleons connected by the Yukawa interaction, Raza et al. investigated ways to extract new, accurate and explicit single soliton solutions related to the nonlinear Klein-Gordon-Schrödinger model [25]. The soliton results of the nonlinear third-order Klein-Fock-Gordon (KFG) problem were invented by Iqbal et al. using the auxiliary equation technique [26]. The equation of relativistic waves associated with NLEEs, the Klein-Fock-Gordon equation (KFGE), was solved by Rehman et al. using the Sardar subequation method (SSM) [27]. The outcomes demonstrate how easy it is to functionalize the SSM to other nonlinear equations. The one-dimensional quadratic Klein-Gordon equation under even perturbations was found to have conditional asymptotic stability in a local energy norm of the unstable soliton by Li and Lührmann [28]. The adiabatic change of the soliton velocity in the presence of perturbation

terms was found by Sassaman and Biswas from the NLKGMs and the phi-four model, three different models with power law nonlinearity of the nonlinear Klein-Gordon equation were examined [29]. Khater et al. used a new generalized analytical scheme to study the computational solutions of the nonlinear Klein-Gordon-Zakharov (KGZ) model [30]. In plasma physics, the evolution of strong Langmuir turbulence is described by this mathematical model. Houwe et al. employed two algorithm integrations the hyperbolic function approach and the $exp(-\phi(\xi))$-expansion method to construct a dark, brilliant, and trigonometric function solution with an M-fractional derivative of order $\alpha$ for the NLKGM [31]. Using the extended tanh approach, Roshid et al. conducted an analytical investigation on soliton, lump wave solution, and rogue waves in the Klein-Gordon with quadratic nonlinearity [32]. This approach possesses complex wave propagation arising in the field of nonlinear optics, theory of quantum field, and solid state physics. The NLKGMs, in the presence of perturbation terms, result in both topological and non-topological solitons, which were explored by Sassaman et al. [33]. Saadatmand and Javidan used various methods to add the inhomogeneities as external potentials to the soliton equation of motion in order to construct the collective-coordinate equations for solitary solutions of the NLKGM [34].

In this study, for the famous well-known NLKGM, Firstly, we have used a renowned method known as sub-ODE method for exact soliton solutions, where we got some soliton solutions as a result of applying sub-ODE to our NLKGM. A bright soliton solution was obtained Eq (2.33), stable and localized wave solutions, bright solitons are essential for a wide range of scientific and technological applications. They function as reliable carriers in fiber optics and telecommunications, enabling distortion-free long-distance signal transmission. Bright solitons are controlled in ultracold atomic gases, especially in Bose-Einstein condensates, to explore quantum phenomena. We have obtained periodic soliton solutions, Eqs (2.35), (2.41), (2.51), and (2.53). Solitons with periodic behavior are called periodic soliton solutions. Periodic soliton solutions occur in systems supporting soliton-like structures with periodic properties in mathematical physics, specifically in the context of (NLPDEs). Studying stress wave propagation in periodic structures is important for material scientists because it helps create materials with desired mechanical and optical characteristics. They are essential for characterizing powerful light pulses in nonlinear optics, which affects the use of mode-locked lasers among other projects. We have obtained a rational soliton solution, Eq (2.37), in mathematics, a rational soliton solution is a kind of solution to NLPDEs, particularly those connected to soliton theory. Rational solitons are associated with rational functions that fulfill the specified nonlinear equation, in contrast to traditional solitons, which are usually defined by solitary wave solutions. A wide range of scientific fields, including physics, optics, and fluid dynamics, have used rational soliton solutions in their respective applications. For the purpose of understanding and predicting complex nonlinear processes in several disciplines of study, rational soliton solutions are useful instruments due to their adaptability. We have derived a dark soliton solution Eq (2.39), solitary wave solutions to (NLPDEs) that describe one-dimensional systems, like the nonlinear Schrödinger equation, are known as dark soliton solutions. Dark solitons are distinct from typical solitons in that they signify isolated areas of lower amplitude or intensity within a higher intensity background. In the area of nonlinear optics, dark solitons have been thoroughly investigated. In this sector, they are used in the control and modification of light pulses in optical fibers. We have obtained Weierstrass elliptic function solution Eq (2.43), two important applications in mathematics and physics involve the doubly periodic complex-valued function known as the Weierstrass elliptic function. Its importance arises from the

fact that it solves the differential equation that characterizes elliptic curves. We have obtained positive soliton solution Eq (2.45). A particular kind of solitary wave in nonlinear systems with a positive amplitude and a localized, self-reinforcing profile is called a positive soliton solution. These solutions are representative of stable, coherent structures that can spread without dispersing and are usually seen in NLPDEs. Positive solitons find significant uses in fluid dynamics and optics, among other domains. We have obtained the hyperbolic function solutions Eqs (2.47) and (2.49). The definition of hyperbolic functions, a class of mathematical functions related to trigonometric functions but not in terms of circles, is in terms of hyperbolas. Among the hyperbolic functions are the hyperbolic tangent (tanh), hyperbolic cosine (cosh), and hyperbolic sine (sinh). Numerous mathematical and scientific applications involve these functions. Hyperbolic functions are commonly found in the solution of differential equations in physics and engineering, which describe a variety of processes like heat conduction, string vibration, and electric circuits.

Secondly, for numerical solutions, we have also studied FDS, by which we determined the solution of the periodic kind of numerical solution, Eq (3.10), by analyzing F-FDS to Eq (1.1). We have also utilized the remaining combinations given in Eq (1.1) as F-BDS to obtain Eq (3.15), F-CDS to obtain Eq (3.20), B-BDS to obtain Eq (3.25), B-FDS to obtain Eq (3.30), B-CDS to obtain Eq (3.35), C-CDS to obtain Eq (3.40), C-FDS to obtain Eq (3.45) and C-BDS to obtain Eq (3.50). Using all the previously stated schemes, numerical 3-D surfaces of the bright type numerical solutions were generated.

At the end, the Lagrangian approach has been used to apply NLKGM. Equation (4.1) represents the Lagrangian for NLKGM. Equation (4.4), in continuous form, gave the Euler Lagrange equation. We created a discrete version of our NLKGM by discretizing Lagrangian density using F-CDS in both time and space, and then we obtained Eq (4.8). Equation (4.9) shows how the time derivative was created using the finite difference. The discrete Euler Lagrange equation, or Eq (4.10), was finally constructed by solving the previous equation for $\wp_t^{n+1}$.

## 6. Conclusions

The sub-ODE approach is used by the NLKGM to obtain soliton solutions. When applying the Lagrangian and finite difference methods, we have obtained the numerical solutions. In this paper, the projection approach was used in all of its conceivable combinations, including F-FDS, F-BDS, F-CDS, B-BDS, B-FDS, B-CDS, C-CDS, C-FDS, C-BDS and so on. Finally, we compared the numerical solutions with the soliton solutions. We also provide contour, 2D, and 3D graphs as a graphical representation of our solutions. A contour plot is a graphic tool that uses contour lines to display a three-dimensional surface on a two-dimensional plane. The function being plotted's constant values are represented by each contour line, thereby mapping the function's value across the plane. A contour plot's geometry displays the surface topography, with lines representing equal-height levels. Closely spaced lines represent steep gradients, whereas widely spaced lines suggest progressive slopes. These lines' spacing and shape reveal information about the gradient and nature of the surface. Plots of contours can show a variety of phenomena, including saddle points—areas where the surface curves in opposite directions and peaks (local maxima) and valleys (local minima). In different fields like geography, engineering, and meteorology, they are frequently used to display complex data in an understandable way. They are especially beneficial for visualizing functions with multiple variables. To the best of our knowledge, these are the first results we have seen for this model. This model for

VIs and FDS is the first time it has been studied. We have also compared the numerical and exact solutions for our governing model. At the end, we have also plotted the "Relative energy error" which also shows the comparison between analytical and numerical solutions. This shows the error is minimum.

## Author contributions

Syed T. R. Rizvi: Supervision, Methodology, Project Administration; Sana Ghafoor: Investigation, Writing-original draft; Aly R. Seadawy: Software, Formal analysis; Ahmed H. Arnous: Validation, Data curation; Hakim AL Garalleh: Resources, Funding Acquisition; Nehad Ali Shah: Review and Editing, Conceptualization. All authors have read and approved the final version of the manuscript for publication.

## Use of AI tools declaration

The authors declare they have not used Artificial Intelligence (AI) tools in the creation of this article.

## Acknowledgments

The authors acknowledge that this project was funded by the Deanship of Scientific Research (DSR), University of Business and Technology, Jeddah 21361, Saudi Arabia. The authors, therefore, gratefully acknowledge the DSR technical and financial support.

## Conflict of interest

The authors declare that they have no competing interests.

## References

1. N. J. Zabusky, M. D. Kruskal, Interaction of solitons in a collisionless plasma and the recurrence of initial states, *Phys. Rev. Lett*, **15** (1965), 240–243. https://doi.org/10.1103/physrevlett.15.240
2. M. T. Darvishi, M. Najafi, L. Akinyemi, H. Rezazadeh, Gaussons of some new nonlinear logarithmic equations, *J. Nonlinear Opt. Phys. Mater.*, **3** (2023), 2350013. https://doi.org/10.1142/s0218863523500133
3. L. Akinyemi, S. Manukure, A. Houwe, S. Abbagari, A study of (2+1)-dimensional variable coefficients equation: Its oceanic solitons and localized wave solutions, *Phys. Fluids*, **36** (2024), 013120. https://doi.org/10.1063/5.0180078
4. L. Akinyemi, M. Şenol, U. Akpan, K. Oluwasegun, The optical soliton solutions of generalized coupled nonlinear Schrödinger-Korteweg-de Vries equations, *Opt. Quan. Electron.*, **53** (2021), 394. https://doi.org/10.1007/s11082-021-03030-7

5. M. Senol, E. A. Az-Zo'bi, L. Akinyemi, A. O. Alleddawi, Novel soliton solutions of the generalized (3+1)-dimensional conformable KP and KP–BBM equations, *Comput. Sci. Eng.*, **1** (2021), 1–29. https://doi.org/10.22124/cse.2021.19356.1003
6. A. Abdeljabba, H. O. Roshid, A. Aldurayhim, Bright, Dark, and Rogue Wave Soliton Solutions of the Quadratic Nonlinear Klein-Gordon Equation, *Symmetry*, **14** (2022), 1223. https://doi.org/10.3390/sym14061223
7. U. Younas, M. Younis, A. R. Seadawy, S. T. R. Rizvi, S. Althobaiti, S. Sayed, Diverse exact solutions for modified nonlinear Schrödinger equation with conformable fractional derivative, *Results Phys.*, **20** (2021), 103766. http://doi.org/10.1016/j.rinp.2020.103766
8. D. D. Santo, T. Kinoshita, M. Reissig, Klein-Gordon type equations with a singular time-dependent potential, *Rend. Istit. Mat. Univ. Trieste*, **XXXIX** (2007), 141–175.
9. Y. V. Bebikhov, I. A. Shepelev, S. V. Dmitriev, A review of specially discretized Klein-Gordon models, *Saratov Fall Meeting 2019: Computations and Data Analysis: From Nanoscale Tools to Brain Functions*, **1145910** (2020), 217–224. https://doi.org/10.1117/12.2565763
10. F. Hirosawa, M. Reissig, From wave to Klein-Gordon type decay rates, In: *Nonlinear Hyperbolic Equations, Spectral Theory, and Wavelet Transformations*, Basel: Birkhäuser, 2003. https://doi.org/10.1007/978-3-0348-8073-2_2
11. C. Böhme, M. Reissig, Energy bounds for Klein-Gordon equations with time-dependent potential, *Ann. Univ. Ferrara*, **59** (2013), 31–55. https://doi.org/10.1007/s11565-012-0162-8
12. E. M. E. Zayed, M. E. M. Alngar, A. Biswas, H. Triki, Y. Yıldırım, A. S. Alshomrani, Chirped and chirp-free optical solitons in fiber Bragg gratings with dispersive reflectivity having quadratic-cubic nonlinearity by sub-ODE approach, *Optik*, **203** (2020), 163993. https://doi.org/10.1016/j.ijleo.2019.163993
13. J. C. Butcher, *Numerical methods for ordinary differential equations*, 2 Eds., Chichester: John Wiley and Sons, 2008. https://doi.org/10.1002/9781119121534
14. B. Leimkuhler, S. Reich, Simulating Hamiltonian dynamics, *Cambridge University Press, Cambridge*, (2004). https://doi.org/10.1017/CBO9780511614118
15. M. Kraus, Projected variational integrators for degenerate Lagrangian systems, 2017. https://doi.org/10.48550/arXiv.1708.07356
16. E. Hairer, C. Lubich, G. Wanner. Geometric Numerical Integration: Structure-Preserving Algorithms for Ordinary Differential Equations. *Springer Series in Computational Mathematics, Springer Berlin, Heidelberg*, 31 2nd edition (2006). https://doi.org/10.1007/3-540-30666-8
17. S. Reich, C. Cotter, Variational integrators and adaptive time stepping for the numerical simulation of wave energy propagation, *J. Comput. Phys.*, **256** (2014), 460–480.
18. A. J. Lew, Discrete variational Hamiltonian mechanics, *Rep. Math. Phys.*, **52** (2003), 147–158.
19. J. C. Butcher, General linear methods, *Acta Numer.*, **15** (2006), 157–256.
20. F. Shehzad, Y. Habib, Discrete Gradient Methods for Solving SIRI Epidemic Model Numerically While Preserving First Integrals, *Arabian J. Sci. Eng.*, **46** (2021), 663–668.
21. J. C. Butcher, Y. Habib, A. T. Hill, T. J. Norton, The control of parasitism in G-symplectic methods, *SIAM J. Numer. Anal*, **52** (2014), 2440–2465.

22. J. E. Marsden, G W. Patrick, The structure and stability of periodic orbits for Hamiltonian systems, *Rep. Prog. Phys.*, **56** (1994), 439.

23. M. Kraus, Variational integrators in plasma physics, 2013. https://doi.org/10.48550/arXiv.1307.5665

24. S. Lall, M. West, Discrete variational Hamiltonian mechanics, *J. Phys. A: Math. General*, **39** (2006), 5509.

25. N. Raza, S. Arshed, A. R. Butt, D. Baleanu, New and more solitary wave solutions for the Klein-Gordon-Schrödinger model arising in nucleon-meson interaction, *Sec. Stat. Comput. Phys.*, **9** (2021), 637964. https://doi.org/10.3389/fphy.2021.637964

26. M. Iqbal, D. Lu, A. R. Seadawy, G. Mustafa, Z. Zhang, M. Ashraf, A. Ghaffar, Dynamical analysis of soliton structures for the nonlinear third-order Klein-Fock-Gordon equation under explicit approach, *Opt. Quant. Electron.*, **56** (2024), 651. https://doi.org/10.1007/s11082-023-05435-y

27. H. U. Rehman, I. Iqbal, S. S. Aiadi, N. Mlaiki, M. S. Saleem, Soliton solutions of Klein-Fock-Gordon equation using sardar subequation method, *Mathematics*, **10** (2022), 3377. https://doi.org/10.3390/math10183377

28. Y. Li, J. Lührmann, Soliton dynamics for the 1D quadratic Klein-Gordon equation with symmetry, *J. Differ. Eq.*, **344** (2023), 172–202. https://doi.org/10.1016/j.jde.2022.10.030

29. R. Sassaman, A. Biswas, Soliton perturbation theory for phi-four model and nonlinear Klein-Gordon equations, *Commun. Nonlinear Sci. Numer. Simul.*, **14** (2009), 3239–3249. https://doi.org/10.1016/j.jfranklin.2010.04.012

30. M. M. A. Khater, A. A. Mousa, M. A. El-Shorbagy, R. A. M. Attia, Abundant novel wave solutions of nonlinear Klein-Gordon-Zakharov (KGZ) model, *Eur. Phys. J. Plus*, **136** (2021), 604. https://doi.org/10.1140/epjp/s13360-021-01385-0

31. A. Houwe, H. Rezazadeh, A. Bekir, S. Y. Doka, Traveling-wave solutions of the Klein-Gordon equations with M-fractional derivative, *Pramana*, **96** (2022), 26. https://doi.org/10.1007/s12043-021-02254-2

32. M. M. Roshid, M. F. Karim, A. K. Azad, M. M. Rahman, T. Sultana, New solitonic and rogue wave solutions of a Klein-Gordon equation with quadratic nonlinearity, *Partial Differ. Eq. Appl. Math.*, **3** (2021), 100036. https://doi.org/10.1016/j.padiff.2021.100036

33. R. Sassaman, A. Heidari, A. Biswas, Topological and non-topological solitons of nonlinear Klein-Gordon equations by He's semi-inverse variational principle, *J. Franklin Inst.*, **347** (2010), 1148–1157. https://doi.org/10.1016/j.jfranklin.2010.04.012

34. D. Saadatmand, K. Javidan, Collective-coordinate analysis of inhomogeneous nonlinear Klein-Gordon Field Theory, *Braz. J. Phys.*, **43** (2013), 48–56. https://doi.org/10.1007/s13538-012-0113-y

AIMS Press